

## Meson-baryon interaction in the hadron exchange picture

M. Döring

**H. Haberzettl, J. Haidenbauer, C. Hanhart, F. Huang, S. Krewald,  
U.-G. Meißner, K. Nakayama, D. Rönchen,**  
Forschungszentrum Jülich, Universität Bonn, University of Georgia, GWU

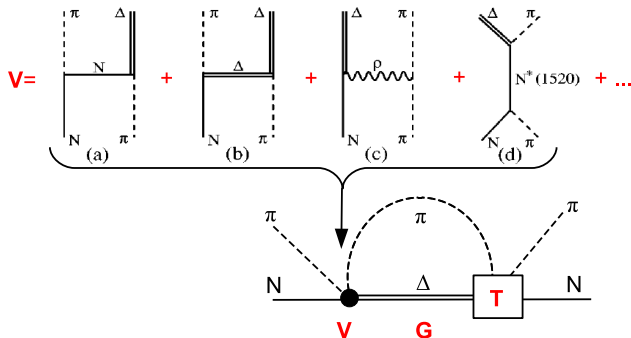
# The Jülich model of pion-nucleon interaction

## Motivation

- Coupled channels  $\pi N$ ,  $\eta N$ ,  $KY$ ; effective  $\pi\pi N$  channels  $\sigma N$ ,  $\rho N$ ,  $\pi\Delta$ .
- Chiral Lagrangian of Wess and Zumino [PR163 (1967), Phys.Rept. 161 (1988)].
- Baryonic resonances up to  $J = 7/2$  with derivative couplings.

## Scattering equation in the $JLS$ basis

$$\langle L' S' k' | T_{\mu\nu}^{IJ} | L S k \rangle = \langle L' S' k' | V_{\mu\nu}^{IJ} | L S k \rangle + \sum_{\gamma, L'' S''} \int_0^{\infty} k''^2 dk'' \langle L' S' k' | V_{\mu\gamma}^{IJ} | L'' S'' k'' \rangle \frac{1}{Z - E_{\gamma}(k'') + i\epsilon} \langle L'' S'' k'' | T_{\gamma\nu}^{IJ} | L S k \rangle$$



Scattering equation in the *JLS* basis

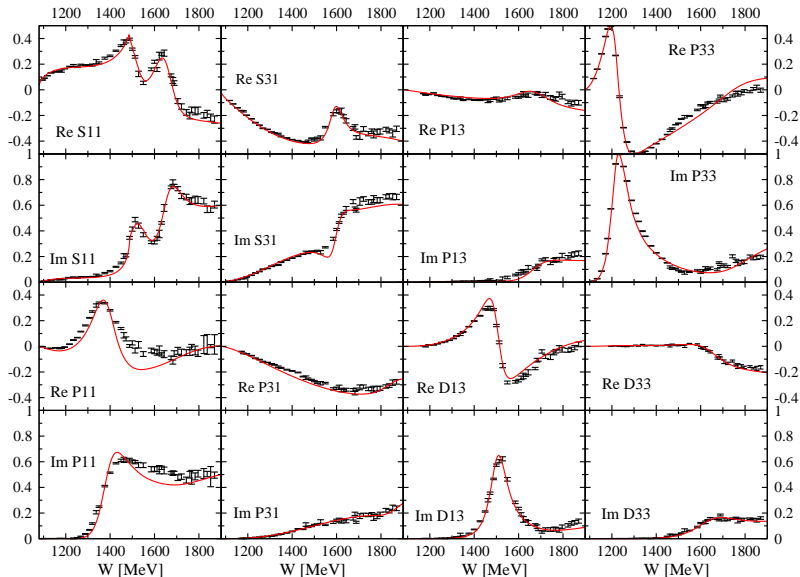
$$\langle L' S' k' | T_{\mu\nu}^{IJ} | L S k \rangle = \langle L' S' k' | V_{\mu\nu}^{IJ} | L S k \rangle + \sum_{\gamma, L'' S''} \int_0^{\infty} k''^2 dk'' \langle L' S' k' | V_{\mu\gamma}^{IJ} | L'' S'' k'' \rangle \frac{1}{Z - E_{\gamma}(k'') + i\epsilon} \langle L'' S'' k'' | T_{\gamma\nu}^{IJ} | L S k \rangle$$

## Features

- Hadron exchange: provides the relevant dynamics.
- Full analyticity (dispersive parts).
- All partial waves are linked (t-, u-channel processes)
- Channels linked (SU(3) symmetry).
- Dynamical generation of resonances is possible, but not easy (strong constraints).

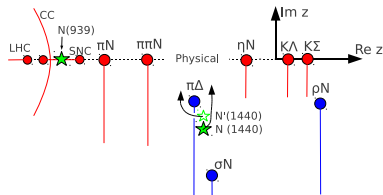
# Partial waves in $\pi N \rightarrow \pi N$ (Solution 2002)

"Data": GWU/SAID, PRC74 (2006)



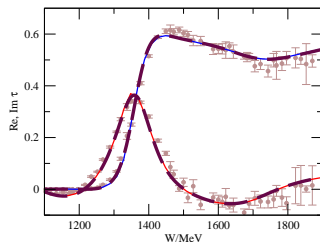
# Structure of the P11 partial wave (Roper)

analytic continuation



- $N(\pi\pi)_{L=I=0}$  channel important (chiral  $\sigma$ ); Roper dynamically generated in Jülich model.
- Roper pole  $N(1440) + \pi\Delta$  branch point  $\rightarrow$  non-standard resonance shape.
- Sub-threshold cuts from crossing symmetry.

- Where is the  $3^* N(1710)$ ?  
[S. Ceci, M.D. et al, arXiv 1104.3490]



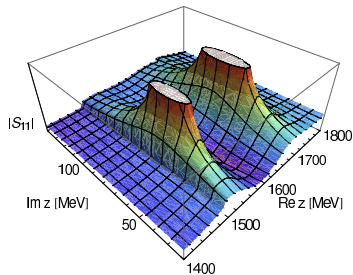
Fit of a model without  $\rho N$  branch point (CMB type) [solid lines] to the Jülich amplitude [dashed lines]

- CMB fit to JM has pole at  $1698 - 130 i$  MeV, simulates missing branch point.
- $\rightarrow$  Inclusion of full analytic structure important to avoid false pole signals.

Branch points in  $\gamma n \rightarrow \eta n$

# Poles and residues

[M.D., C. Hanhart, F. Huang, S. Krewald and U.-G. Meißner, NPA 829 (2009), PLB 681 (2009)]



	Re $z_0$ [MeV]	-2 Im $z_0$ [MeV]	$ R $ [MeV]	$\theta$ [deg] [ $^{\circ}$ ]
$N^*(1535) S_{11}$	1519	129	31	-3
ARN	1502	95	16	-16
HOE	1487			
CUT	1510±50	260±80	120±40	+15±45
$N^*(1650) S_{11}$	1669	136	54	-44
ARN	1648	80	14	-69
HOE	1670	163	39	-37
CUT	1640±20	150±30	60±10	-75±25
$N^*(1720) P_{13}$	1663	212	14	-82
ARN	1666	355	25	-94
HOE	1686	187	15	
CUT	1680±30	120±40	8±12	-160±30
$\Delta(1232) P_{33}$	1218	90	47	-37
ARN	1211	99	52	-47
HOE	1209	100	50	-48
CUT	1210±1	100±2	53±2	-47±1
$\Delta^*(1620) S_{31}$	1593	72	12	-108
ARN	1595	135	15	-92
HOE	1608	116	19	-95
CUT	1600±15	120±20	15±2	-110±20
$\Delta^*(1700) D_{33}$	1637	236	16	-38
ARN	1632	253	18	-40
HOE	1651	159	10	
CUT	1675±25	220±40	13±3	-20±25
$N^*(1440) P_{11}$	1387	147	48	-64
ARN	1359	162	38	-98
HOE	1385	164	40	
CUT	1375±30	180±40	52±5	-100±35
$N^*(1520) D_{13}$	1505	95	32	-18
ARN	1515	113	38	-5
HOE	1510	120	32	-8
CUT	1510±5	114±10	35±2	-12±5
$\Delta^*(1910) P_{31}$	1840	221	12	-153
ARN	1771	479	45	+172
HOE	1874	283	38	
CUT	1880±30	200±40	20±4	-90±30

[ARN]: Arndt et al., PRC 74 (2006), [HOE]: Höhler,  $\pi N$  Newsl. 9 (1993), [CUT]: Cutkowski et al., PRD 20 (1979).

Residues to  $\eta N$ ,  $\sigma N$ ,  $\rho N$ ,  $\pi \Delta$ . Zeros. Branching ratios to  $\pi N$ ,  $\eta N$ .

## The reaction $\pi^+ p \rightarrow K^+ \Sigma^+$

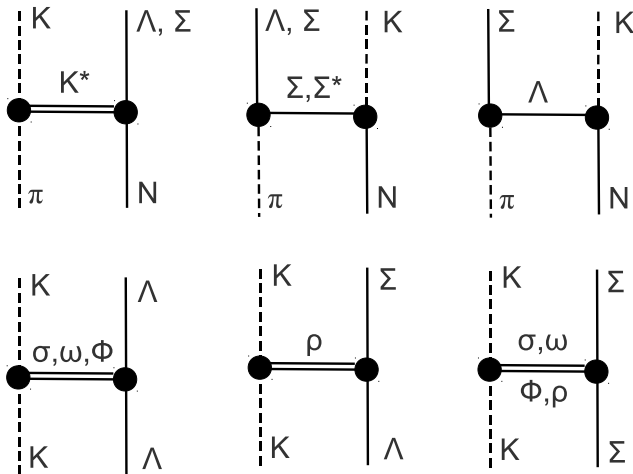
Towards a unified analysis of different final states

- From the example of the  $N(1710)P_{11}$ : different reaction channels provide more information on resonance content than higher precision in one channel.
- SU(3) symmetry provides predictive power.
- $\pi^+ p \rightarrow K^+ \Sigma^+$ : Pure isospin 3/2; relatively few  $\Delta$  resonances.
- Simultaneous fit to  $\pi N \rightarrow \pi N$  partial waves [energy dependent GWU SAID solution, PRC74 (2006)] plus  $\pi^+ p \rightarrow K^+ \Sigma^+$  observables.
- Guiding principle in the fit: Resonances are the last resort (while technically being the easiest way to improve the  $\chi^2$ ).
- Error analysis on pole positions is crucial.



## Inclusion of the $KY$ channels

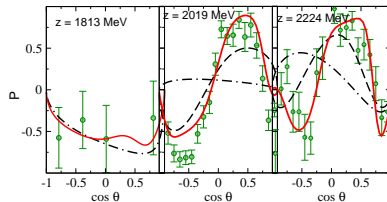
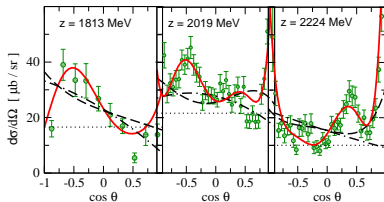
Inclusion via  $SU(3)$  symmetry **plus  $s$ -channel resonance vertices to  $KY$  (not shown; 40 parms.)**.



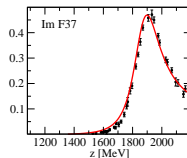
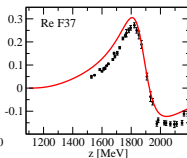
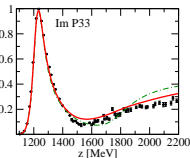
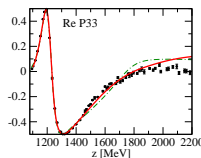
# The reaction $\pi^+ p \rightarrow K^+ \Sigma^+$

M.D., C. Hanhart, F. Huang, S. Krewald, U.-G. Meißner, D. Rönchen, [NPA851 (2011)]

[Link to full Results & Error analysis](#)



Data upper: Candlin 1983, NPB 226 (1983), lower: GWU/SAID, PRC74 (2006)



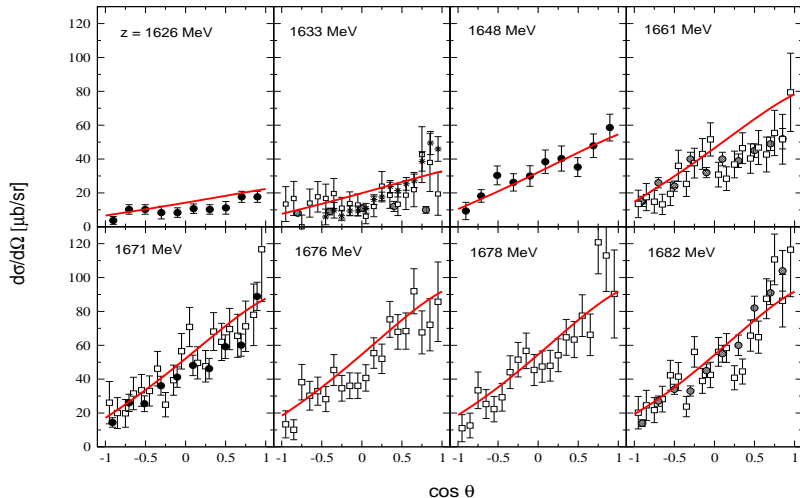
Linking partial waves and **different reactions** puts more constraints on

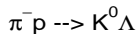
resonance content

# Example of other final states [preliminary, no $N(1710)P11$ needed so far]

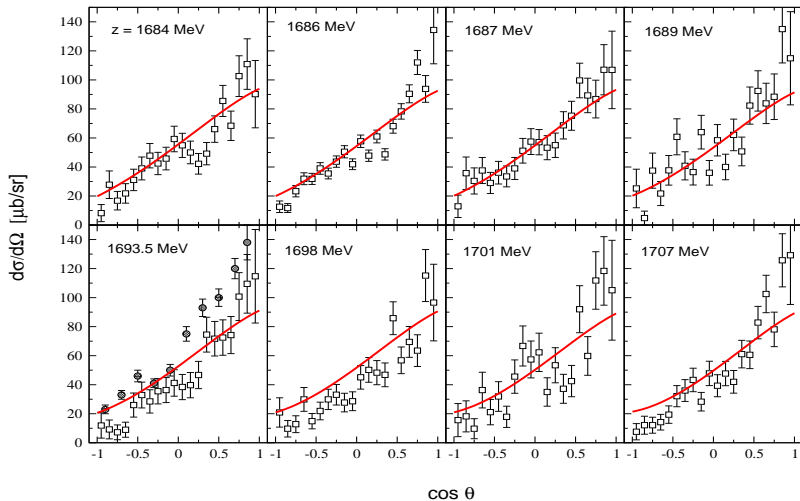
$$\pi^- p \rightarrow K^0 \Lambda$$

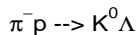
- Bertanaz 62, PRL 8, 332
- Baker 78 NPB 141, 29
- Knasel 75 PR11,1
- \* Yoder 63, PR 132, 1778



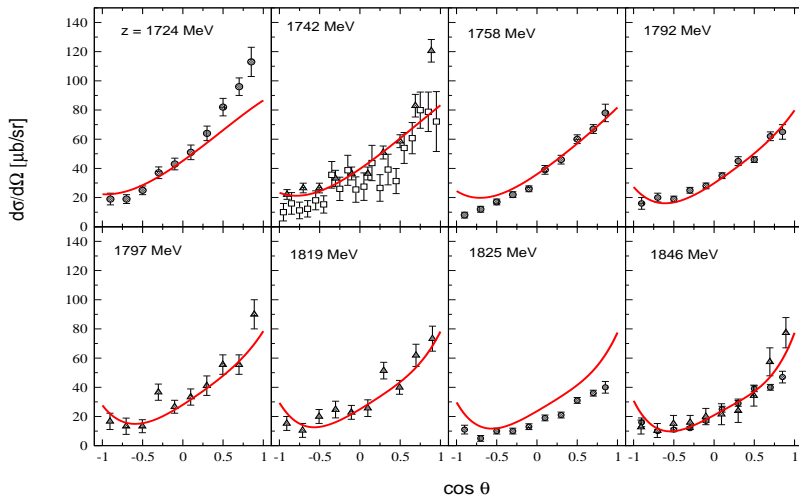


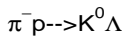
- Knasel 75, PRD 11,1
- Baker 78, NPB 141,29



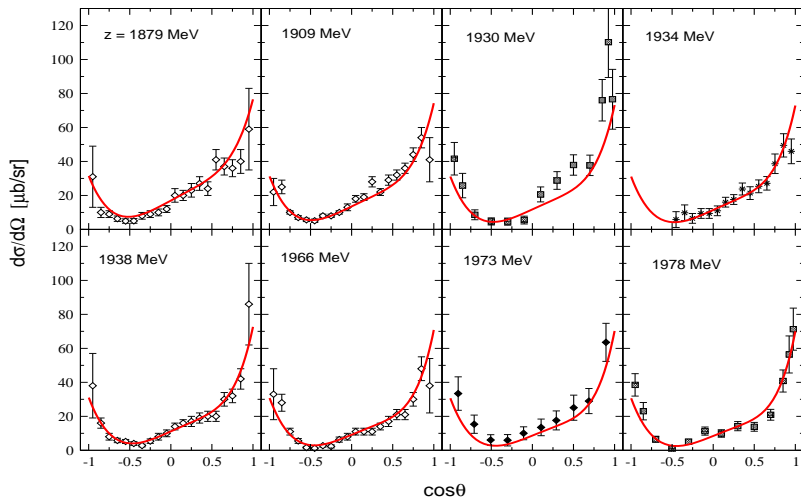


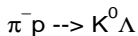
- ▲ Binford 69 PR 183,1134
- Knasel 75 PRD 11,1
- Baker 78 NPB 141,29



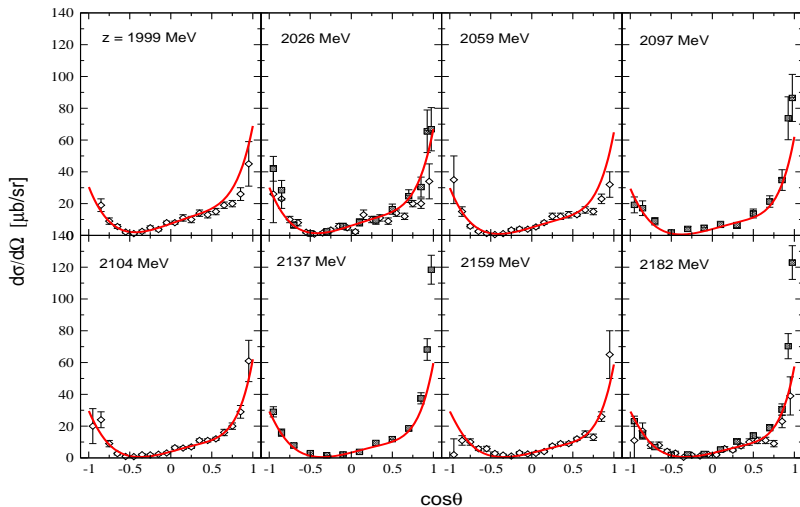


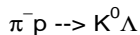
- \* Yoder 63, PRL 132, 1778
- ◆ Goussu 66, NCA 42, 607
- ◇ Saxon 80, NPB 162,522
- Dahl 67, PR 163, 1430



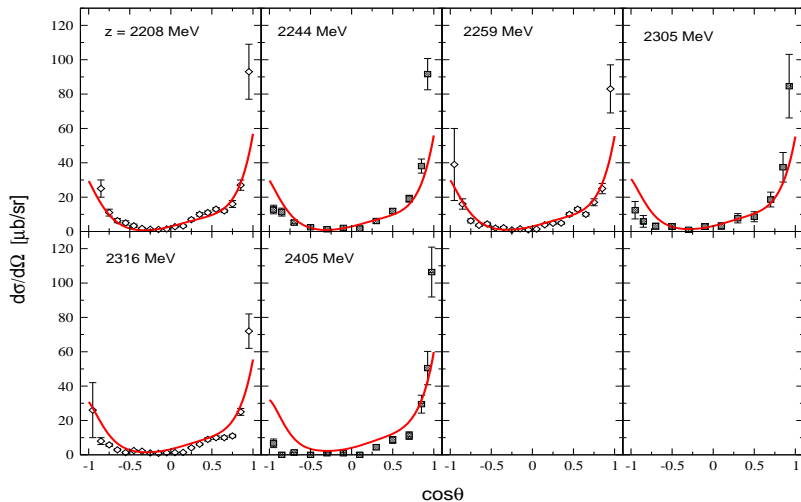


- Dahl 67, PR 163, 1430
- ◇ Saxon 80 NPB 162, 522





- ◇ Saxon 80, NPB 162, 522
- Dahl 67, PR 163, 1430



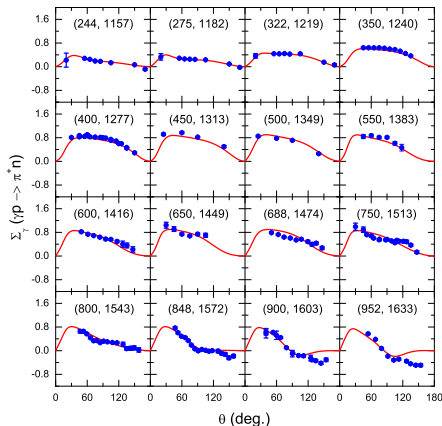
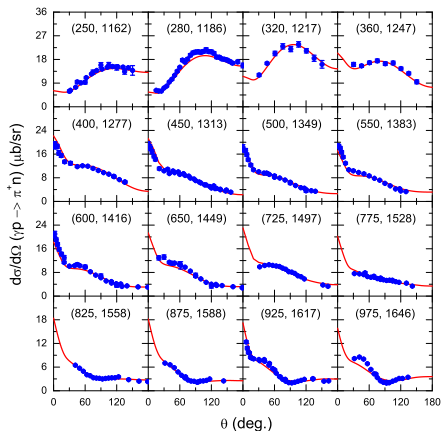


# Linking reactions: $d\sigma/d\Omega$ and $\Sigma_\gamma$ for $\gamma p \rightarrow \pi^+ n$

F. Huang, K. Nakayama, M.D., *et al.*, in prep. (see also arXiv:1103.2065)

Gauge invariance respected

Further results  $\gamma N \rightarrow \pi N$



Differential cross section for  $\gamma p \rightarrow \pi^+ n$

Data: CNS Data analysis center [CBELSA/TAPS, JLAB, MAMI,...]

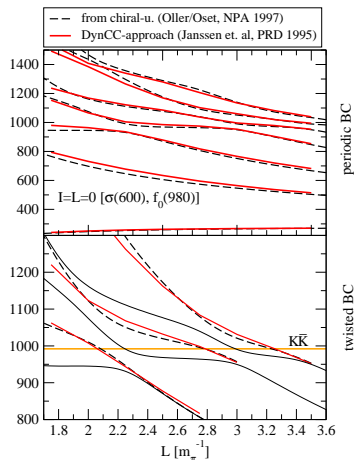
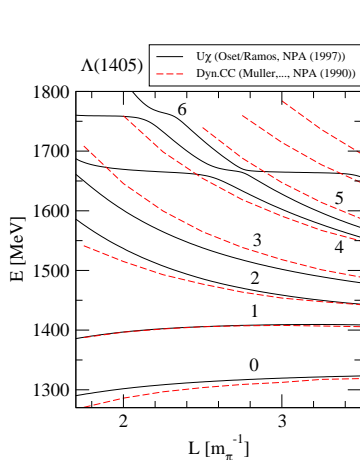
Photon spin asymmetry for  $\gamma p \rightarrow \pi^+ n$

# Dynamical coupled channels models in a box

Discretization & twisted BC

[M.D., J. Haidenbauer, A. Rusetsky, U.-G. Meißner, E. Oset, in preparation]

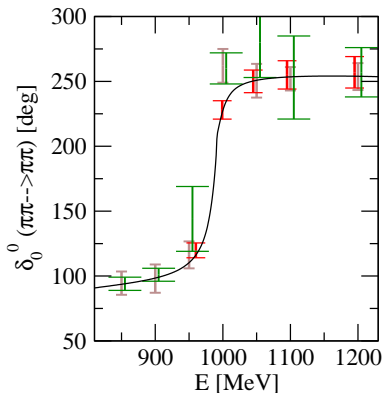
- Variation of box size  $L \rightarrow$  reconstruction of phase shifts (Lüscher)
- Examples:  $\Lambda(1405)$ ,  $\sigma(600)$ ,  $f_0(980)$  on the lattice.
- Prediction of lattice levels & including coming lattice-data in analysis.



## Multi-channel dynamics

Error propagation from pseudo lattice-data [M.D., U.-G. Meißner, E. Oset, A. Rusetsky, in prep.]

- Coupled channels  $\pi\pi, \bar{K}K$ :  
 three unknowns
  - $V(\pi\pi \rightarrow \pi\pi)$
  - $V(\pi\pi \rightarrow \bar{K}K)$
  - $V(\bar{K}K \rightarrow \bar{K}K)$
- How good is the reconstructed phase shift using different lattice data?
- Use pseudo-data generated from hadronic model.
- Hadronic input can reduce the error.



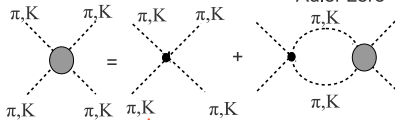
- red: twisted boundary conditions
- green: Asymmetric boxes
- brown: different levels

## Conclusions

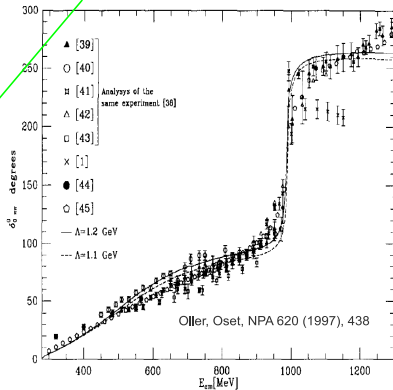
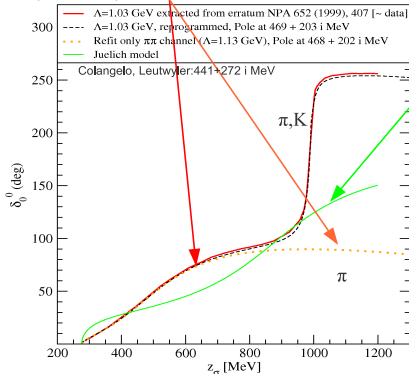
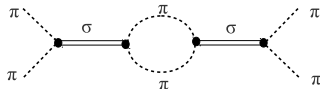
- Lagrangian based, field theoretical description of meson-baryon interaction. Unitarity and analyticity are ensured.
- Meson and baryon exchange are the relevant degrees of freedom in the 2<sup>nd</sup> and 3<sup>rd</sup> resonance region. Exchange provides constraints, because all partial waves are linked. With this background, only a few bare states are needed (cleaner resonance extraction).
- $\Rightarrow$  precise determination of model independent resonance parameters (poles).
- Branch points in the complex plane/on the real axis may lead to false resonance signals. Different reaction channels provide more information on resonance content than higher precision in one only.
- Coupled channel formalism links different reactions in one combined description:
  - $\pi N \rightarrow \pi N, \pi N \rightarrow \eta N, KY, \dots, \gamma N \rightarrow \pi N, \dots$
- Dynamical coupled channel models on a momentum lattice (predict levels, error propagation, analyse coming lattice data).

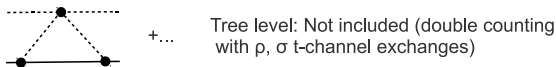
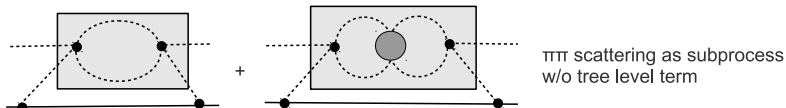
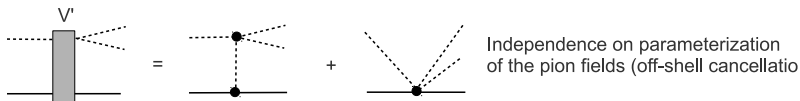
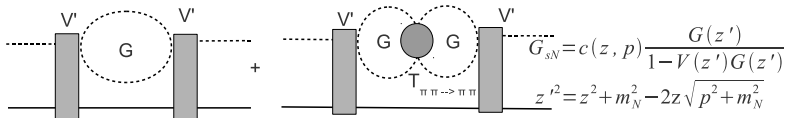
# Chiral unitary approach to $\pi\pi$ scattering

$$T_{\pi\pi} = V_\chi + V_\chi G T_{\pi\pi}; \quad V_\chi = \underbrace{(1/2m_\pi^2 - s)}_{\text{Adler zero}} / f^2$$



$$T_{\pi\pi} = (V_{\sigma\pi\pi})^2 / (z - M - \Sigma_{\pi\pi})$$





# Analytic continuation via Contour deformation

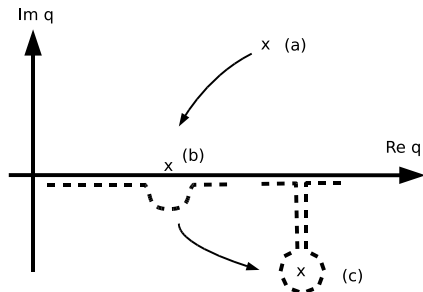
...enables access to all Riemann sheets

$$\Pi_{\sigma}(z) = \int_0^{\infty} q^2 dq \frac{(v^{\sigma\pi\pi}(q))^2}{z - E_1 - E_2 + i\epsilon}$$

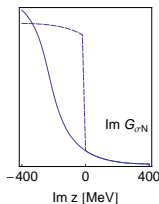
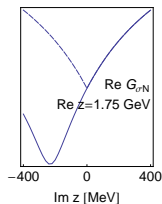
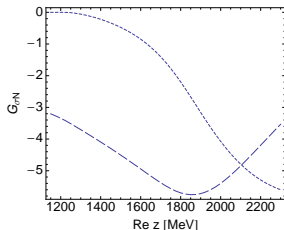
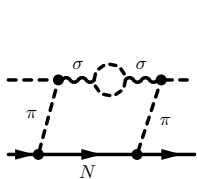
$$z - E_1 - E_2 = 0 \Leftrightarrow q = q_{c.m.}$$

$$q_{c.m.} = \frac{1}{2z} \sqrt{[z^2 - (m_1 - m_2)^2][z^2 - (m_1 + m_2)^2]}$$

- Plot  $q_{c.m.}(z)$  in the  $q$  plane of integration (X: Pole positions).
- case (a),  $\text{Im } z > 0$ : straight integration from  $q = 0$  to  $q = \infty$ .
- case (b),  $\text{Im } z = 0$ : Pole is on real  $q$  axis.
- case (c),  $\text{Im } z < 0$ : Deformation gives analytic continuation.
- Special case: Pole at  $q = 0$   
 $\Leftrightarrow$  branch point at  $z = m_1 + m_2$  (= threshold).



# Propagator of effective $\pi\pi N$ channels $\sigma N$ , $\rho N$ , $\pi\Delta$

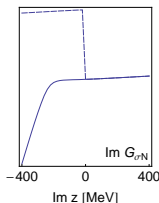
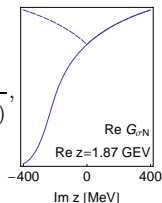


$$g_{\sigma N}(z, k) =$$

$$\frac{1}{z - \sqrt{m_N^2 + k^2} - \sqrt{(m_\sigma^0)^2 + k^2} - \Pi_\sigma(z_\sigma(z, k), k)},$$

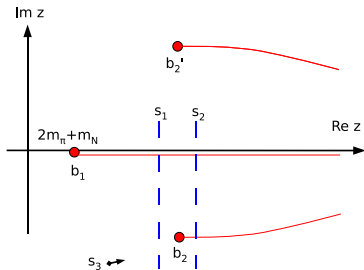
$$G_{\sigma N}(z) = \int_0^\infty dk k^2 F(k) g_{\sigma N}(z, k),$$

$$z_\sigma(z, k) = z + m_\sigma^0 - \sqrt{k^2 + (m_\sigma^0)^2} - \sqrt{k^2 + m_N^2}$$

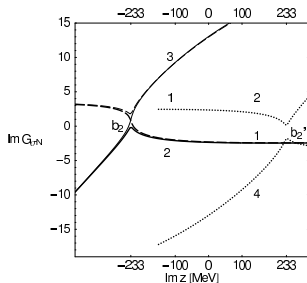


→ Branch point in the complex  $z$  plane.



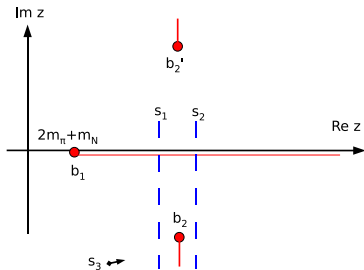


Three branch points and four sheets for each of the  $\sigma N$ ,  $\rho N$ , and  $\pi\Delta$  propagators.



- The cut along  $\text{Im } z = 0$  is induced by the cut of the self energy of the unstable particle.
- The poles of the unstable particle ( $\sigma$ ) induce branch points in the  $\sigma N$  propagator at

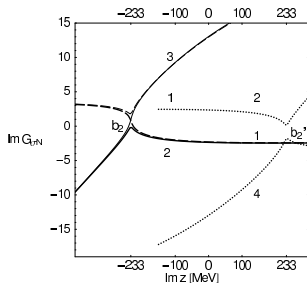
$$z_{b_2} = m_N + z_0, \quad z_{b_2'} = m_N + z_0^*$$



Three branch points and four sheets for each of the  $\sigma N$ ,  $\rho N$ , and  $\pi\Delta$  propagators.

- The cut along  $\text{Im } z = 0$  is induced by the cut of the self energy of the unstable particle.
- The poles of the unstable particle ( $\sigma$ ) induce branch points in the  $\sigma N$  propagator at

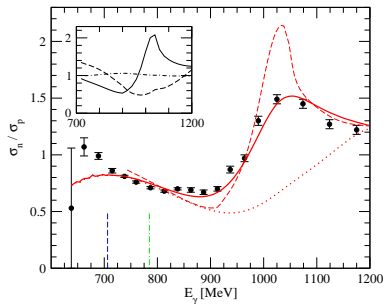
$$z_{b_2} = m_N + z_0, \quad z_{b_2'} = m_N + z_0^*$$



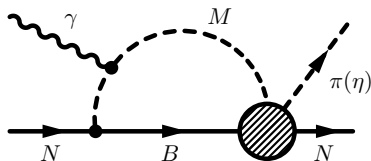
# Branch points in coupled channels ( $\gamma N \rightarrow \eta N$ )

[M.D., K. Nakayama, EPJA43 (2010), PLB683 (2010)]

◀ back



[Data: I. Jaegle et al., CBELSA/TAPS, PRL 100 (2008)]

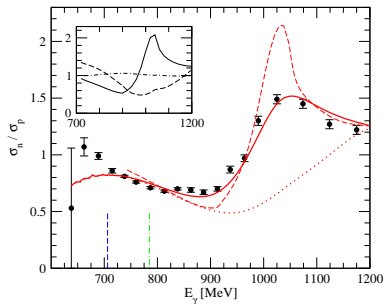


- $MB = \pi N, \eta N, K\Lambda, K\Sigma$
- Pronounced cusp from dispersive (“real”) part of the loop.
- Analyticity is crucial.

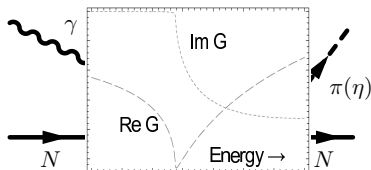
# Branch points in coupled channels ( $\gamma N \rightarrow \eta N$ )

[M.D., K. Nakayama, EPJA43 (2010), PLB683 (2010)]

◀ back



[Data: I. Jaegle et al., CBELSA/TAPS, PRL 100 (2008)]



- $MB = \pi N, \eta N, K\Lambda, K\Sigma$
- Pronounced cusp from dispersive (“real”) part of the loop.
- Analyticity is crucial.

	$N\pi$	$N\rho^{(1)} (S = 1/2)$	$N\rho^{(2)} (S = 3/2)$	$N\rho^{(3)} (S = 3/2)$
$N^*(1535) S_{11}$	$S_{11} \quad 8.1 + 0.5i$	$S_{11} \quad 2.2 - 5.4i$	–	$D_{11} \quad 0.5 - 0.3i$
$N^*(1650) S_{11}$	$S_{11} \quad 8.6 - 2.8i$	$S_{11} \quad 0.9 - 9.1i$	–	$D_{11} \quad 0.3 - 0.1i$
$N^*(1440) P_{11}$	$P_{11} \quad 11.2 - 5.0i$	$P_{11} \quad -1.3 + 3.2i$	$P_{11} \quad 3.6 - 2.6i$	–
$\Delta^*(1620) S_{31}$	$S_{31} \quad 2.9 - 3.7i$	$S_{31} \quad 0.0 - 0.0i$	–	$D_{31} \quad 0.0 - 0.0i$
$\Delta^*(1910) P_{31}$	$P_{31} \quad 1.2 - 3.5i$	$P_{31} \quad 0.2 - 0.4i$	$P_{31} \quad -0.2 - 0.4i$	–
$N^*(1720) P_{13}$	$P_{13} \quad 3.7 - 2.6i$	$P_{13} \quad 0.1 + 0.8i$	$P_{13} \quad -1.1 + 0.1i$	$F_{13} \quad 0.1 - 0.1i$
$N^*(1520) D_{13}$	$D_{13} \quad 8.4 - 0.8i$	$D_{13} \quad -0.6 + 0.7i$	$D_{13} \quad 0.9 - 2.0i$	$S_{13} \quad -2.5 - 0.5i$
$\Delta(1232) P_{33}$	$P_{33} \quad 17.9 - 3.2i$	$P_{33} \quad -1.3 - 0.8i$	$P_{33} \quad -0.9 - 3.0i$	$F_{33} \quad 0.0 - 0.0i$
$\Delta^*(1700) D_{33}$	$D_{33} \quad 4.9 - 1.0i$	$D_{33} \quad -0.2 + 0.9i$	$D_{33} \quad -0.4 - 0.4i$	$S_{33} \quad -0.1 - 0.1i$

	$N\eta$	$\Delta\pi^{(1)}$	$\Delta\pi^{(2)}$	$N\sigma$
$N^*(1535) S_{11}$	$S_{11} \quad 11.9 - 2.3i$	–	$D_{11} \quad -5.9 + 4.8i$	$P_{11} \quad -1.4 - 0.4i$
$N^*(1650) S_{11}$	$S_{11} \quad -3.0 + 0.5i$	–	$D_{11} \quad 4.3 + 0.4i$	$P_{11} \quad -2.1 - 0.1i$
$N^*(1440) P_{11}$	$P_{11} \quad -0.1 + 0.0i$	$P_{11} \quad -4.6 - 1.7i$	–	$S_{11} \quad -8.3 - 0.3i$
$\Delta^*(1620) S_{31}$	–	–	$D_{31} \quad 11.1 - 4.0i$	–
$\Delta^*(1910) P_{31}$	–	$P_{31} \quad 15.0 - 0.3i$	–	–
$N^*(1720) P_{13}$	$P_{13} \quad -7.7 + 5.5i$	$P_{13} \quad -14.1 + 3.0i$	$F_{13} \quad 0.0 - 0.3i$	$D_{13} \quad -0.8 - 0.8i$
$N^*(1520) D_{13}$	$D_{13} \quad 0.16 - 0.60i$	$D_{13} \quad 0.0 + 0.4i$	$S_{13} \quad -12.9 - 0.7i$	$P_{13} \quad -0.6 - 0.6i$
$\Delta(1232) P_{33}$	–	$P_{33} \quad -(4 \text{ to } 5) + i(0 \text{ to } 0.5)$	$F_{33} \quad \sim 0$	–
$\Delta^*(1700) D_{33}$	–	$D_{33} \quad -0.7 - 0.3i$	$S_{33} \quad -19.7 + 4.5i$	–

Resonance couplings  $g_i$  [ $10^{-3} \text{ MeV}^{-1/2}$ ] to the coupled channels  $i$ . Also, the  $LJS$  type of each coupling is indicated. For the  $\rho N$  channels, the total spin  $S$  is also indicated.

first sheet	second sheet	[FA02]
$P_{11}$ 1235 - 0 $i$	$S_{11}$ 1587 - 45 $i$	1578 - 38 $i$
$D_{33}$ 1396 - 78 $i$	$S_{31}$ 1585 - 17 $i$	1580 - 36 $i$
	$P_{31}$ 1848 - 83 $i$	1826 - 197 $i$
	$P_{13}$ 1607 - 38 $i$	1585 - 51 $i$
	$P_{33}$ 1702 - 64 $i$	-
	$D_{13}$ 1702 - 64 $i$	1759 - 64 $i$

Position of **zeros** of the full amplitude  $T$  in [MeV]. [FA02]: Arndt et al., PRC 69 (2004).

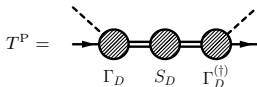
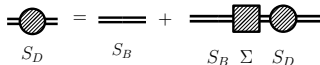
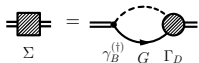
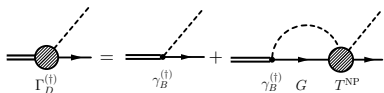
	$\Gamma_{\pi N}/\Gamma_{\text{Tot}}$ [%]	$\Gamma_{\eta N}/\Gamma_{\text{Tot}}$ [%]
$N^*(1535) S_{11}$	48 [33 to 55]	38 [45 to 60]
$N^*(1650) S_{11}$	79 [60 to 95]	6 [3 to 10]
$N^*(1440) P_{11}$	64 [55 to 75]	0 [0 $\pm$ 1]
$\Delta^*(1620) S_{31}$	34 [20 to 30]	-
$\Delta^*(1910) P_{31}$	11 [15 to 30]	-
$N^*(1720) P_{13}$	13 [10 to 20]	38 [4 $\pm$ 1]
$N^*(1520) D_{13}$	67 [55 to 65]	0.10 [0.23 $\pm$ 0.04]
$\Delta(1232) P_{33}$	100 [100]	-
$\Delta^*(1700) D_{33}$	13 [10 to 20]	-

**Branching ratios** into  $\pi N$  and  $\eta N$ . The values in brackets are from the PDG, [Amsler et al., PLB 667 (2008)].

# Couplings and dressed vertices

Residue  $a_{-1}$  vs. dressed vertex  $\Gamma$  vs. bare vertex  $\gamma$ .

◀ back



$$a_{-1} = \frac{\Gamma_d \Gamma_d^{(\dagger)}}{1 - \frac{\partial}{\partial Z} \Sigma}$$

$$g = \sqrt{a_{-1}}$$

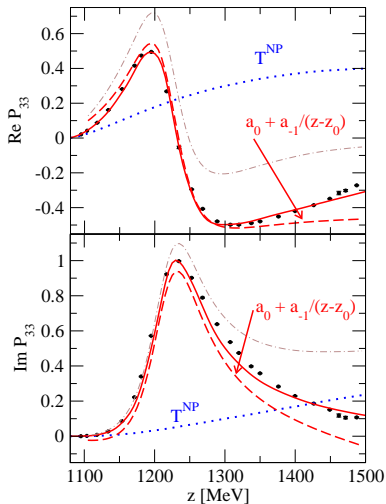
$$r = |(\Gamma_D - \gamma_B)/\Gamma_D|,$$

$$r' = |1 - \sqrt{1 - \Sigma'}|,$$

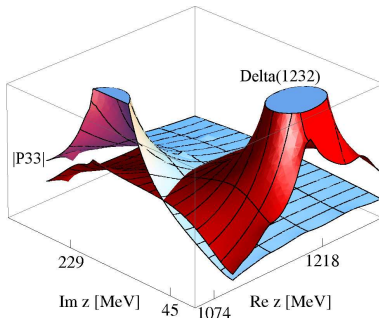
- Dressed  $\Gamma$  depends on  $T^{NP}$ .

$$\boxed{\sqrt{a_{-1}} \neq \Gamma \neq \gamma}$$

	$\gamma^C$	$\Gamma^C$	$r$ [%]	$r'$ [%]
$N^*(1520) D_{13}$	$6.4 - 0.6i$	$13.2 + 1.2i$	53	61
$N^*(1720) P_{13}$	$-0.1 + 5.4i$	$0.9 + 4.8i$	24	45
$\Delta(1232) P_{33}$	$1.3 + 13.0i$	$-2.8 + 22.2i$	45	40
$\Delta^*(1620) S_{31}$	$0.1 + 14.3i$	$5.0 + 5.7i$	130	66
$\Delta^*(1700) D_{33}$	$5.4 - 0.8i$	$6.7 + 1.0i$	33	54
$\Delta^*(1910) P_{31}$	$9.4 + 0.3i$	$1.9 - 3.2i$	222	22



- Poles in  $T^{\text{NP}}$  may occur  $\Rightarrow$  pole repulsion in  $T = T^{\text{NP}} + T^{\text{P}}$ !





$g_{fi}$  und  $h_{fi}$  in JLS-Basis:

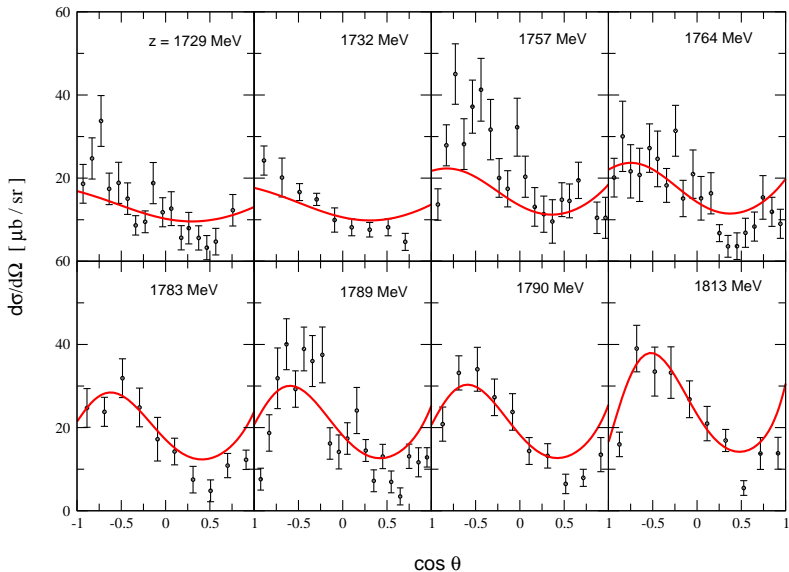
$$g_{fi} = \frac{1}{2\sqrt{k_f k_i}} \sum_j (2j+1) d_{\frac{1}{2}\frac{1}{2}}^j(\theta) \left[ \tau^{j(j-\frac{1}{2})\frac{1}{2}} + \tau^{j(j+\frac{1}{2})\frac{1}{2}} \right] \cos \frac{\theta}{2} \\ + \frac{1}{2\sqrt{k_f k_i}} \sum_j (2j+1) d_{-\frac{1}{2}\frac{1}{2}}^j(\theta) \left[ \tau^{j(j-\frac{1}{2})\frac{1}{2}} - \tau^{j(j+\frac{1}{2})\frac{1}{2}} \right] \sin \frac{\theta}{2}$$

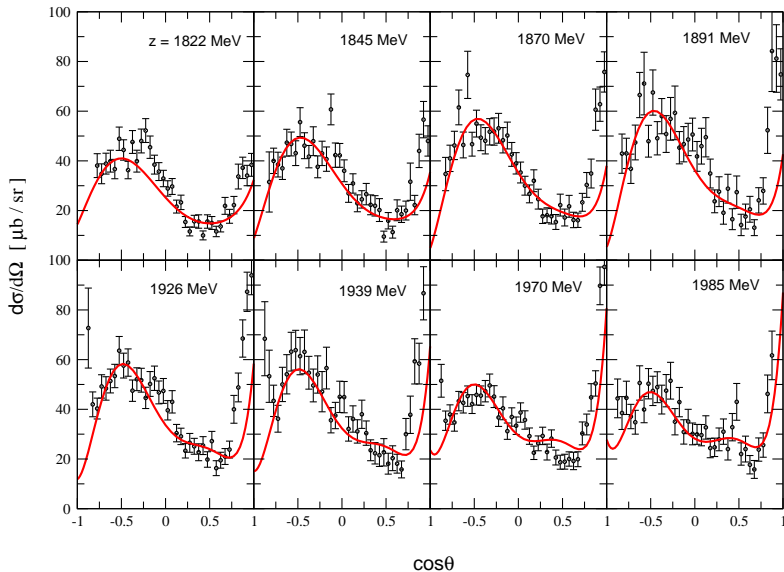
$$h_{fi} = \frac{-i}{2\sqrt{k_f k_i}} \sum_j (2j+1) d_{\frac{1}{2}\frac{1}{2}}^j(\theta) \left[ \tau^{j(j-\frac{1}{2})\frac{1}{2}} + \tau^{j(j+\frac{1}{2})\frac{1}{2}} \right] \sin \frac{\theta}{2} \\ + \frac{i}{2\sqrt{k_f k_i}} \sum_j (2j+1) d_{-\frac{1}{2}\frac{1}{2}}^j(\theta) \left[ \tau^{j(j-\frac{1}{2})\frac{1}{2}} - \tau^{j(j+\frac{1}{2})\frac{1}{2}} \right] \cos \frac{\theta}{2}$$

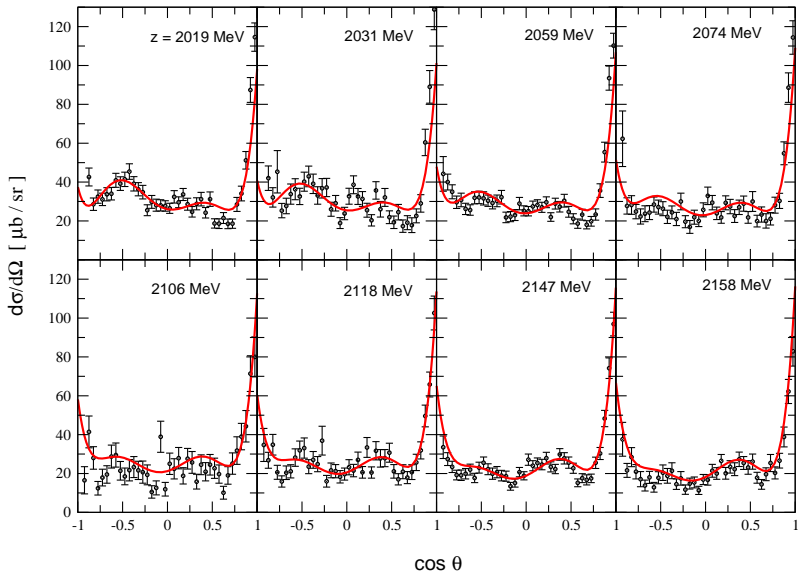
$$\begin{aligned}
 \frac{d\sigma}{d\Omega} &= \frac{k_f}{k_i} (|g_{fi}|^2 + |h_{fi}|^2) \\
 &= \frac{1}{2k_i^2} \frac{1}{2} \cdot \left( \left| \sum_j (2j+1) (\tau^{j(j-\frac{1}{2})\frac{1}{2}} + \tau^{j(j+\frac{1}{2})\frac{1}{2}}) \cdot d_{\frac{1}{2}\frac{1}{2}}^j(\Theta) \right|^2 \right. \\
 &\quad \left. + \left| \sum_j (2j+1) (\tau^{j(j-\frac{1}{2})\frac{1}{2}} - \tau^{j(j+\frac{1}{2})\frac{1}{2}}) \cdot d_{-\frac{1}{2}\frac{1}{2}}^j(\Theta) \right|^2 \right)
 \end{aligned}$$

$$\vec{P}_f = \frac{2\text{Re}(g_{fi}h_{fi}^*)}{|g_{fi}|^2 + |h_{fi}|^2} \cdot \hat{n}$$

$$\beta = \arctan \left( \frac{2\text{Im}(h_{fi}^*g_{fi})}{|g_{fi}|^2 - |h_{fi}|^2} \right)$$

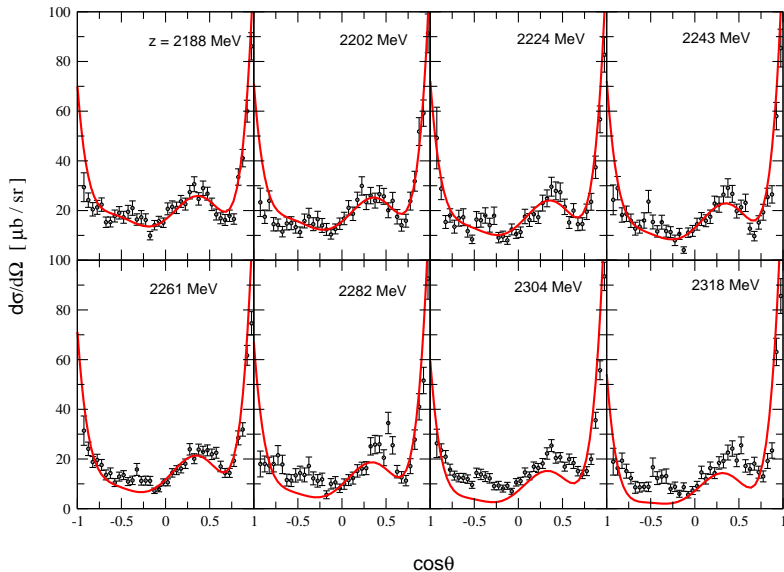




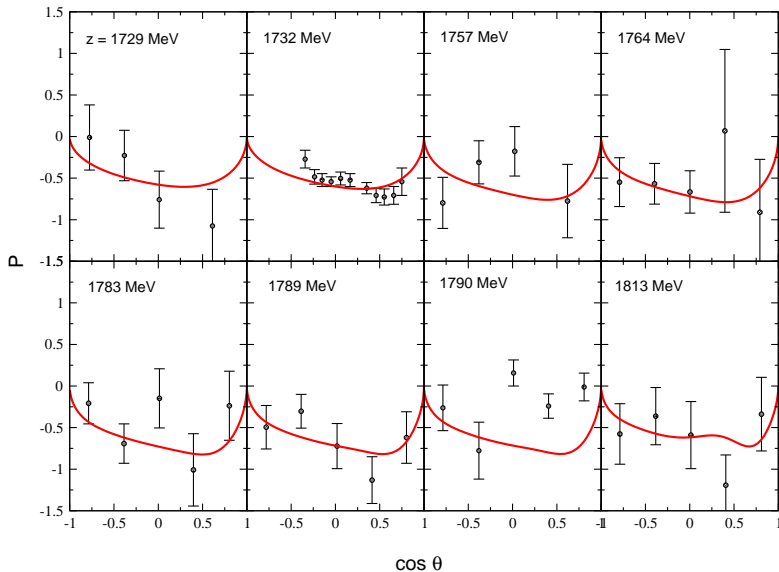


# Differential cross section of $\pi^+ p \rightarrow K^+ \Sigma^+$

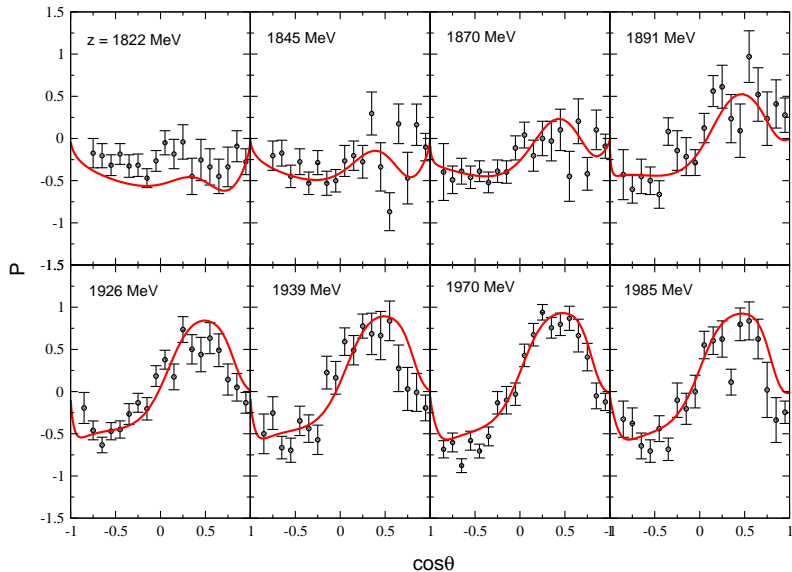
◀ back



# Polarization of $\pi^+ p \rightarrow K^+ \Sigma^+$

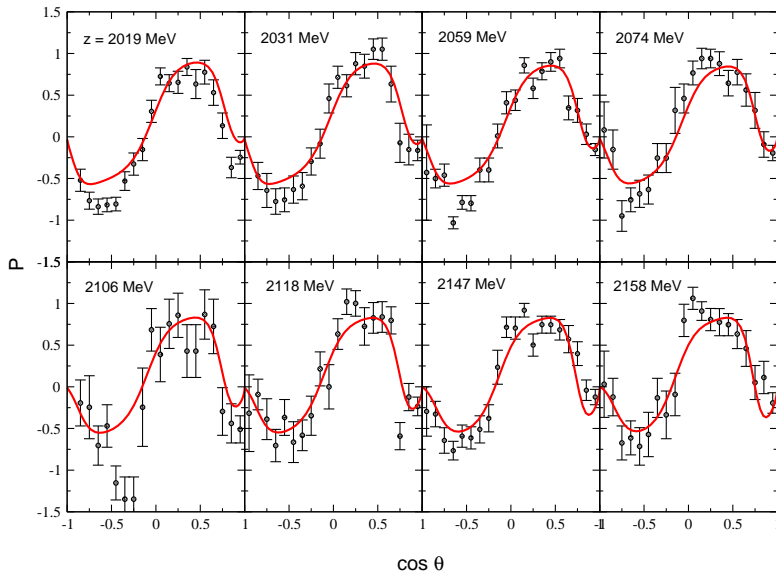


# Polarization of $\pi^+ p \rightarrow K^+ \Sigma^+$

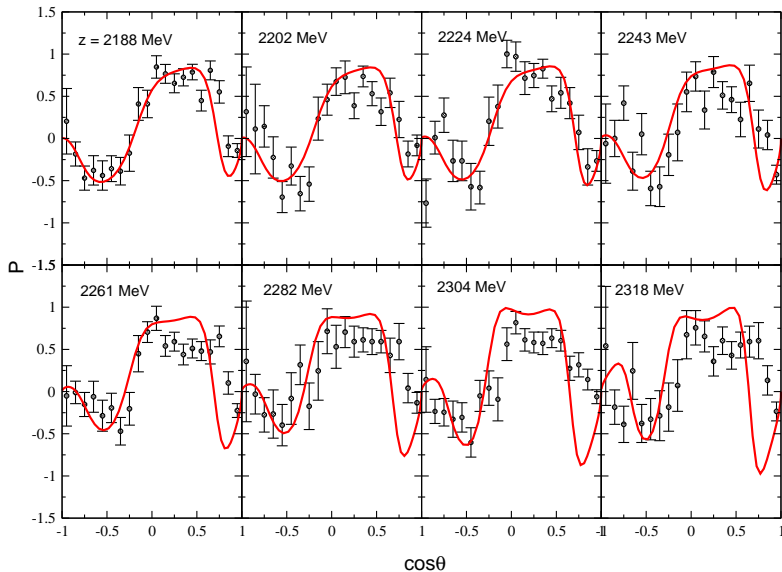




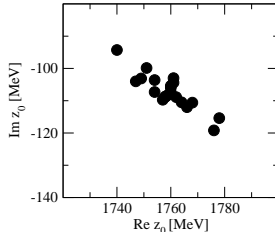
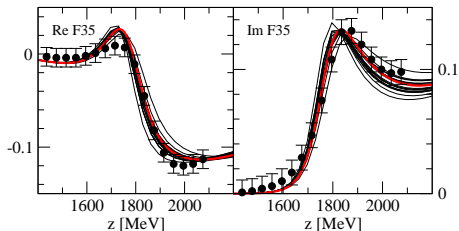
# Polarization of $\pi^+ p \rightarrow K^+ \Sigma^+$



# Polarization of $\pi^+ p \rightarrow K^+ \Sigma^+$



- Determination of the non-linear parameter error
  - $\chi^2 + 1$  criterion.
  - Varying 39 of 40 parameters to get parameter error.
- Get error on derived quantities like pole positions and residues.
- So far, simplified consideration (error from  $\pi N$  not available, because energy dependent GWU/SAID solution is fitted [PRC74 (2006)]).



## Error estimates for parameters and derived quantities

**Table:** Error estimates of bare mass  $m_b$  and bare coupling  $f$  for the  $\Delta(1905)F_{35}$  resonance.

$m_b$ [MeV]	$\pi N$	$\rho N$	$\pi\Delta$	$\Sigma K$
$2258_{-43}^{+44}$	$0.0500_{-0.0012}^{+0.0011}$	$-1.62_{-1.61}^{+1.29}$	$-1.15_{-0.022}^{+0.030}$	$0.120_{-0.0059}^{+0.0065}$

**Table:** Error estimates of pole position and residues for the  $\Delta(1905)F_{35}$  resonance.

			$\pi N \rightarrow \pi N$	$\pi N \rightarrow K\Sigma$
Re $z_0$ [MeV]	$1764_{-20}^{+18}$	$ r $ [MeV]	$11_{-1.4}^{+1.7}$	$1.4_{-0.21}^{+0.24}$
Im $z_0$ [MeV]	$-109_{-12}^{+13}$	$\theta$ [ $^\circ$ ]	$-45_{-11}^{+3.8}$	$-313_{-10}^{+4.2}$

	Re $z_0$ [MeV]	$ r $ [MeV]	$(\Gamma_{\pi N}^{1/2} \Gamma_{K\Sigma}^{1/2}) / \Gamma_{\text{tot}}$ [%]		
	-2 Im $z_0$ [MeV]		$\theta$ [ $^\circ$ ]	This study	Candlin (1983)
$\Delta(1905) F_{35}$	1764	1.4	1.23	1.5(3)	<1
5/2 <sup>+</sup> ****	218	-313			
$\Delta(1910) P_{31}$	1721	5.5	2.98	<3	1.1
1/2 <sup>+</sup> ****	323	-6			
$\Delta(1920) P_{33}$	1884	5.9	5.07	5.2(2)	2.1(3)
3/2 <sup>+</sup> ***	229	-38			
$\Delta(1930) D_{35}$	1865	1.6	2.14	<1.5	
5/2 <sup>-</sup> ***	147	-43			
$\Delta(1950) F_{37}$	1873	2.7	2.54	5.3(5)	—
7/2 <sup>+</sup> ****	206	-255			

# Coupled channels and gauge invariance

Haberzettl, PRC56 (1997), Haberzettl, Nakayama, Krewald, PRC74 (2006),

◀ back

Hadronic scattering:

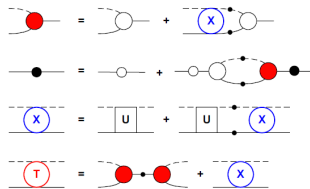
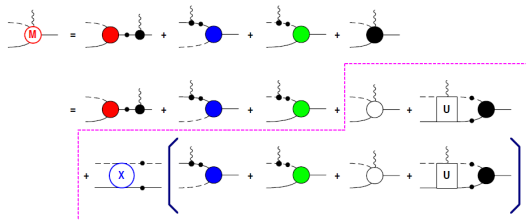


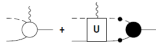
Photo-production:



**Gauge invariance:** Generalized Ward-Takahashi identity (WTI)

(Note the condition of current conservation  $k_\mu M^\mu = 0$  is necessary but not sufficient!)

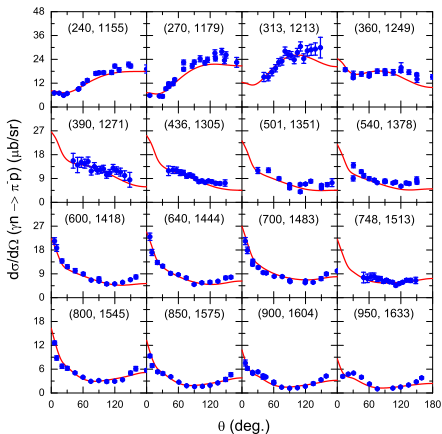
$$k_\mu M^\mu = -|F_s \tau\rangle S_{p+k} Q_i S_p^{-1} + S_{p'}^{-1} Q_f S_{p'-k} |F_u \tau\rangle + \Delta_{p-p'+k}^{-1} Q_\pi \Delta_{p-p'} |F_t \tau\rangle$$

**Strategy:** Replace  by phenomenological contact term such that the generalized WTI is satisfied

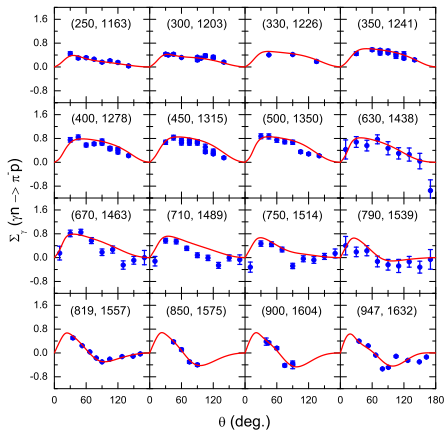
# $d\sigma/d\Omega$ and $\Sigma_\gamma$ for $\gamma n \rightarrow \pi^- p$

preliminary

◀ back



Differential cross section for  $\gamma n \rightarrow \pi^- p$

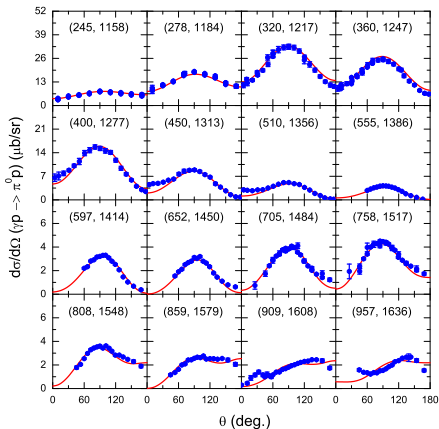


Photon spin asymmetry for  $\gamma n \rightarrow \pi^- p$

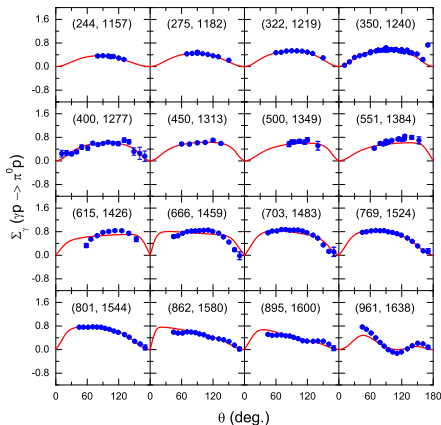
# $d\sigma/d\Omega$ and $\Sigma_\gamma$ for $\gamma p \rightarrow \pi^0 p$

preliminary

◀ back



Differential cross section for  $\gamma p \rightarrow \pi^0 p$



Photon spin asymmetry for  $\gamma p \rightarrow \pi^0 p$



Discretization of momenta in the scattering equation:

$$T(q'', q') = V(q'', q') + \int_0^\infty dq q^2 V(q'', q) \frac{1}{z - E_1(q) - E_2(q) + i\epsilon} T(q, q')$$

$$\int \frac{\vec{d}^3 q}{(2\pi)^3} f(|\vec{q}|^2) \rightarrow \frac{1}{L^3} \sum_{\vec{n}_i} f(|\vec{q}_i|^2), \quad \vec{q}_i = \frac{2\pi}{L} \vec{n}_i, \quad \vec{n}_i \in \mathbb{Z}^3$$

$$T(q'', q') = V(q'', q') + \frac{2\pi^2}{L^3} \sum_{i=0}^\infty \vartheta(i) V(q'', q_i) \frac{1}{z - E_1(q_i) - E_2(q_i)} T(q_i, q'),$$

- Can be also expressed in terms of the Lüscher  $\mathcal{Z}_{00}$  function up to  $e^{-L}$  relativistic corrections.
- Takes into account discretization effects of the potentials themselves.
- Twisted boundary conditions, e.g.

$$u(\mathbf{x} + L\mathbf{e}_i) = u(\mathbf{x}), \quad d(\mathbf{x} + L\mathbf{e}_i) = d(\mathbf{x}), \quad s(\mathbf{x} + L\mathbf{e}_i) = e^{i\theta} s(\mathbf{x}),$$

especially suited for coupled-channels problem (enables to move thresholds) [V. Bernard, M. Lage, U.-G. Meißner, A. Rusetsky, JHEP (2011)].

